Functional equivalence of the clathrin heavy chains CHC17 and CHC22 in endocytosis and mitosis

Fiona E. Hood and Stephen J. Royle*

The Physiological Laboratory, School of Biomedical Sciences, University of Liverpool, Crown Street, Liverpool L69 3BX, UK
*Author for correspondence (e-mail: s.j.royle@liverpool.ac.uk)

Accepted 23 March 2009
Journal of Cell Science 122, 2185-2190 Published by The Company of Biologists 2009
doi:10.1242/jcs.046177

Summary

Clathrin is crucial for endocytosis and plays a recently described role in mitosis. Two clathrin heavy chains (CHCs) are found in humans: the ubiquitous CHC17, and CHC22, a CHC that is enriched in skeletal muscle. Functional differences have been proposed for these clathrins despite high sequence similarity. Here, we compared each paralogue in functional assays of endocytosis and mitosis. We find that CHC17 and CHC22 are functionally equivalent. We also describe how previous work on CHC22 has involved a splice variant that is not usually expressed in cells.

Supplementary material available online at
http://jcs.biologists.org/cgi/content/full/122/13/2185/DC1

Key words: Cell cycle, Clathrin, Endocytosis, Mitosis

Journal of Cell Science

Introduction

Clathrin is a triskelion comprising three clathrin heavy chains (CHCs), each with an associated light chain (Kirchhausen, 2000). Clathrin is crucial for membrane trafficking, particularly for endocytosis at the plasma membrane. It is also proposed to have a role in stabilising fibres of the spindle apparatus during mitosis (Royle, 2006). In humans, there are two isoforms of CHC, which are encoded by separate genes (Wakeham et al., 2005). The first gene (*CLTC*), on chromosome 17, encodes CHC17, which is ubiquitously expressed and has been intensively studied. The second (*CLTCL1*), on chromosome 22, codes for CHC22, a homologue of CHC17 whose function is unclear. CHC22 is expressed at very low levels in most tissues but has a higher expression in skeletal muscle (Gong et al., 1996; Kedra et al., 1996; Lindsay et al., 1996; Long et al., 1996; Sirotkin et al., 1996; Liu et al., 2001). This expression is upregulated during myogenesis, suggesting a role for CHC22 in muscle repair and regeneration (Liu et al., 2001; Towler et al., 2004b).

CHC17 and CHC22 are very similar, with 85% identity (97% similarity) at the amino acid level. However, recent work has suggested that the functions of CHC17 and CHC22 are different. CHC22 appears to be unable to bind AP2, the main adaptor protein for clathrin-mediated endocytosis, but is able to bind other APs (Liu et al., 2001). This has led to the suggestion that CHC22 is not involved in clathrin-mediated endocytosis but in other forms of intracellular trafficking (Towler et al., 2004a). In apparent disagreement with this idea, a recent study has found that CHC22 is a component of clathrin-coated vesicles (CCVs) (Borner et al., 2006). Furthermore, biochemical work has shown that CHC22 cannot bind clathrin light chains, unlike CHC17 (Liu et al., 2001). However, an interaction between clathrin light chain b (LCb) and both CHCs was detected by a yeast two-hybrid assay (Towler et al., 2004b). On balance, the published results represent some confusion over what differences, if any, exist between CHC17 and CHC22.

During mitosis, clathrin becomes associated with the microtubules of the mitotic spindle (Maro et al., 1985; Okamoto et al., 2000; Royle et al., 2005), where it apparently stabilises kinetochore fibres. This has been well documented for CHC17 (Royle et al., 2005; Royle and Lagnado, 2006), but it is untested whether CHC22 also binds to the spindle.

We set out to compare the functions of CHC17 and CHC22 in endocytosis and mitosis in mammalian cells. Our strategy was to express each protein on a background of CHC17-depletion. We found that CHC17 and CHC22 are functionally equivalent. During the course of this work we also established that some of the previous work on CHC22 has been carried out using an incorrect clone that is non-functional in the assays we have used.

Results and Discussion

The subcellular localisation of GFP-tagged CHC22 was examined in mitotic cells. We used a cDNA encoding CHC22 that is the basis for much of the previous work on CHC22 (Liu et al., 2001; Towler et al., 2004b). When expressed in HEK293 cells, this GFP-CHC22 construct, unlike GFP-CHC17, did not associate with the mitotic spindle (Fig. 1). This difference between CHC22 and CHC17 was unexpected given the extensive similarity between the two proteins. In order to determine the region responsible for this difference, we generated six chimeric clathrins using CHC17 and CHC22 (Fig. 1C-H). To our surprise, we found that the region of non-equivalence was located between residues 291-728. This was puzzling owing to our previous observation that the N-terminal domain (residues 1-330) of CHC17 is required for spindle-binding (Royle et al., 2005). The chimeric clathrins in Fig. 1C,D show that the N-terminal domain of CHC17 was not sufficient to confer spindle-binding to CHC22, yet the N-terminal domain from CHC22 could be substituted for that of CHC17 and the resultant chimera was competent for binding. One possible explanation for these results is that the non-equivalence of residues 291-728 is due to an ‘inhibitory sequence’ in CHC22 that prevents triskelia containing this region from binding to the mitotic spindle.

Upon further work to narrow down the region of non-equivalence, we found that the cDNA encoding CHC22 that we used was a variant that lacked exon 9. Exon 9 is a 153-bp exon that codes for residues

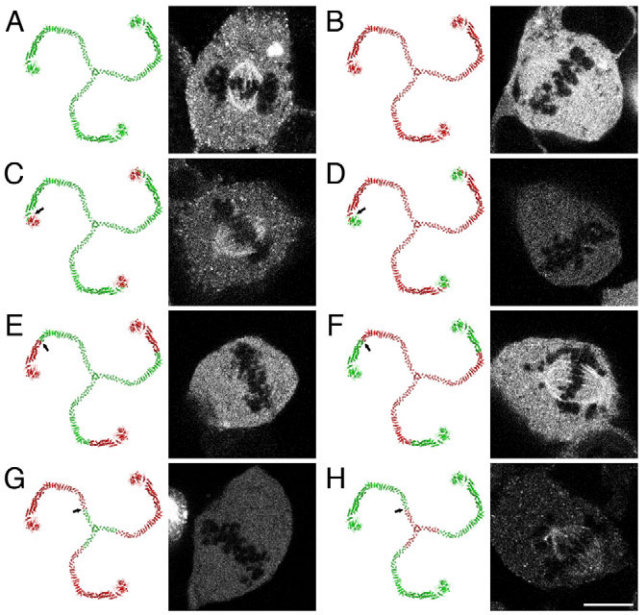

Fig. 1. Recruitment of chimeric clathrin constructs to the mitotic spindle. Representative confocal micrographs of HEK293 cells expressing GFP-tagged clathrin constructs. Schematic diagrams (left in each panel) show the arrangement of CHC17 (green) and CHC22 (red); arrows in C-F indicate changeover points. (A) GFP-CHC17(1-1675); (B) GFP-CHC22(1-1640); (C) GFP-CHC22(1-290)CHC17(291-1675); (D) GFP-CHC17(1-291)CHC22(292-1640); (E) GFP-CHC22(1-728)CHC17(729-1675); (F) GFP-CHC17(1-728)CHC22(729-1640); (G) GFP-CHC22(1-1393)CHC17(1394-1675); (H) GFP-CHC17(1-1393)CHC22(1394-1640). The GFP-CHC22 clone used in these experiments was a variant lacking exon 9 (CHC22ΔExon9). The lack of exon 9 correlated with a lack of spindle recruitment (B,D,E,G). Scale bar: 10 μm.

457-507. These amino acids correspond to helices e-h in CHCR0 (supplementary material Fig. S1). Because the exon 9 residues are within the region of non-equivalence that we had identified, we postulated that the lack of these residues caused the inhibition of spindle-binding. To test this idea, we generated a full-length, exon-9-containing GFP-tagged cDNA encoding CHC22 and expressed it in HEK293 cells. Fig. 2A shows the subcellular distributions of the full-length and exon-skipped forms of CHC22. The full-length form had a subcellular distribution that was similar to that of CHC17. Full-length CHC22 was able to bind to the mitotic spindle and, in interphase cells, had a distribution typical of clathrin: numerous coated pits and vesicles throughout the cell with a perinuclear accumulation around the Golgi complex (Fig. 2A, compare CHC22-FL with CHC17-FL). By contrast, the exon-skipped form (CHC22ΔExon9), which was not recruited to the mitotic spindle, had a diffuse, non-punctate distribution in interphase cells. In addition, we artificially removed exon 9 from CHC17 (CHC17ΔExon9) in order to test the effect of removing these residues in a better-studied clathrin. Fig. 2A shows that CHC17ΔExon9, similar to CHC22ΔExon9, was no longer recruited to the spindle; however, by contrast, CHC17ΔExon9 was still found in an interphase distribution that was similar to full-length CHC17 and CHC22 (CHC17-FL and CHC22-FL, respectively). These results demonstrate that residues encoded by exon 9 are required for localisation of CHCs to the mitotic spindle.

We next wanted to determine the cellular functions of these clathrins. In order to gain a fair comparison of protein function, we expressed each clathrin in HEK293 cells depleted of CHC17. This allowed us to compare the functions of CHC17 and CHC22 directly, without the complication of endogenous CHC17.

We first tested the mitotic function of these clathrins. RNA interference (RNAi) of CHC17 causes chromosome-congression defects that result in prolonged mitosis. This can be measured as an increase in the frequency of metaphase-like cells with misaligned

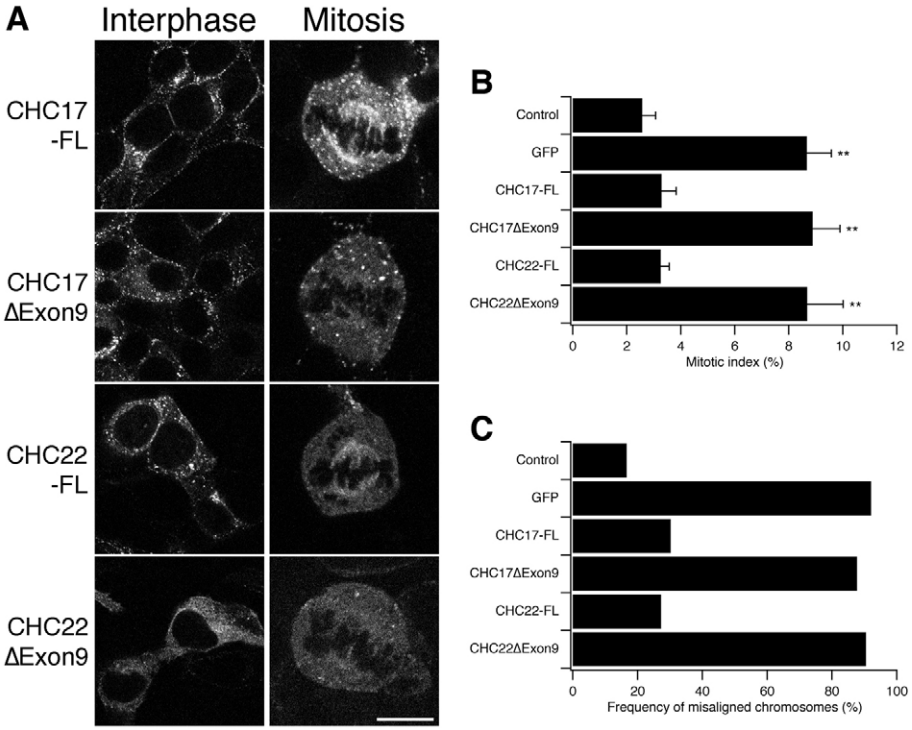

Fig. 2. Rescue of normal mitosis in CHC17-depleted cells by full-length CHC17 or CHC22. (A) Residues 457-507 (exon 9) are necessary for recruitment of CHC17 or CHC22 to the mitotic spindle. Representative confocal micrographs of CHC17-depleted HEK293 cells expressing GFP-tagged clathrin constructs in either interphase (left) or mitosis (right). Scale bar: 20 μm for interphase cells, 10 μm for mitotic cells. (B) Histogram to show mean ± s.d. mitotic index; n=3, $^{**}P<0.01$. (C) Histogram to show the mean frequency of misaligned chromosomes in metaphase-like cells. Results shown are from a typical experiment; n=1. 'Control' is GFP expressed on a control RNAi background. The remainder express the indicated GFP-tagged construct on a CHC17 RNAi background.

chromosomes and an increase in the mitotic index (Royle et al., 2005). We tested for functional rescue of normal mitosis by expressing the clathrins on a background of CHC17 RNAi. We found that CHC17-FL and CHC22-FL were able to fully rescue normal mitosis in CHC17-depleted cells (Fig. 2B,C). CHC17ΔExon9 and CHC22ΔExon9 were unable to rescue normal mitosis, as assessed by there being no significant change in the mitotic index and the frequency of misaligned chromosomes in metaphase-like cells compared with the negative rescue control (GFP) (Fig. 2B,C). These results are consistent with the observation that the exon-skipped forms of CHC17 and CHC22 were unable to bind to the mitotic spindle.

We next tested the function of these clathrin constructs in endocytosis (Fig. 3). We found that CHC17-FL and CHC22-FL were able to rescue transferrin uptake in CHC17-depleted cells to levels similar to those seen in the control RNAi condition (Control) (Fig. 3B). We saw very little transferrin uptake with CHC22ΔExon9; however, CHC17ΔExon9 was able to mediate endocytosis (Fig. 3A,B). The ventral surface of CHC17-depleted cells expressing these clathrins was imaged by confocal microscopy (Fig. 3A). This allowed us to visualise individual transferrin–Alexa-Fluor-546 puncta that colocalise with these clathrins. We could clearly visualise transferrin in CHC22-positive spots, presumably CHC22-coated vesicles, whereas little or no association between CHC22ΔExon9 and transferrin puncta, which were reduced in number, was found (Fig. 3A).

The CHC22-mediated endocytosis described here is in agreement with other work demonstrating that CHC22 is a component of CCVs (Borner et al., 2006). However, previous work had suggested that endogenous CHC22 that was immunoprecipitated from HeLa cells did not associate with AP2, unlike CHC17 (Liu et al., 2001). The mode of AP-binding by the CHC17 N-terminal domain is well-defined (Dell'Angelica et al., 1998; ter Haar et al., 2000; Drake and Traub, 2001; Miele et al., 2004), and all of the residues involved

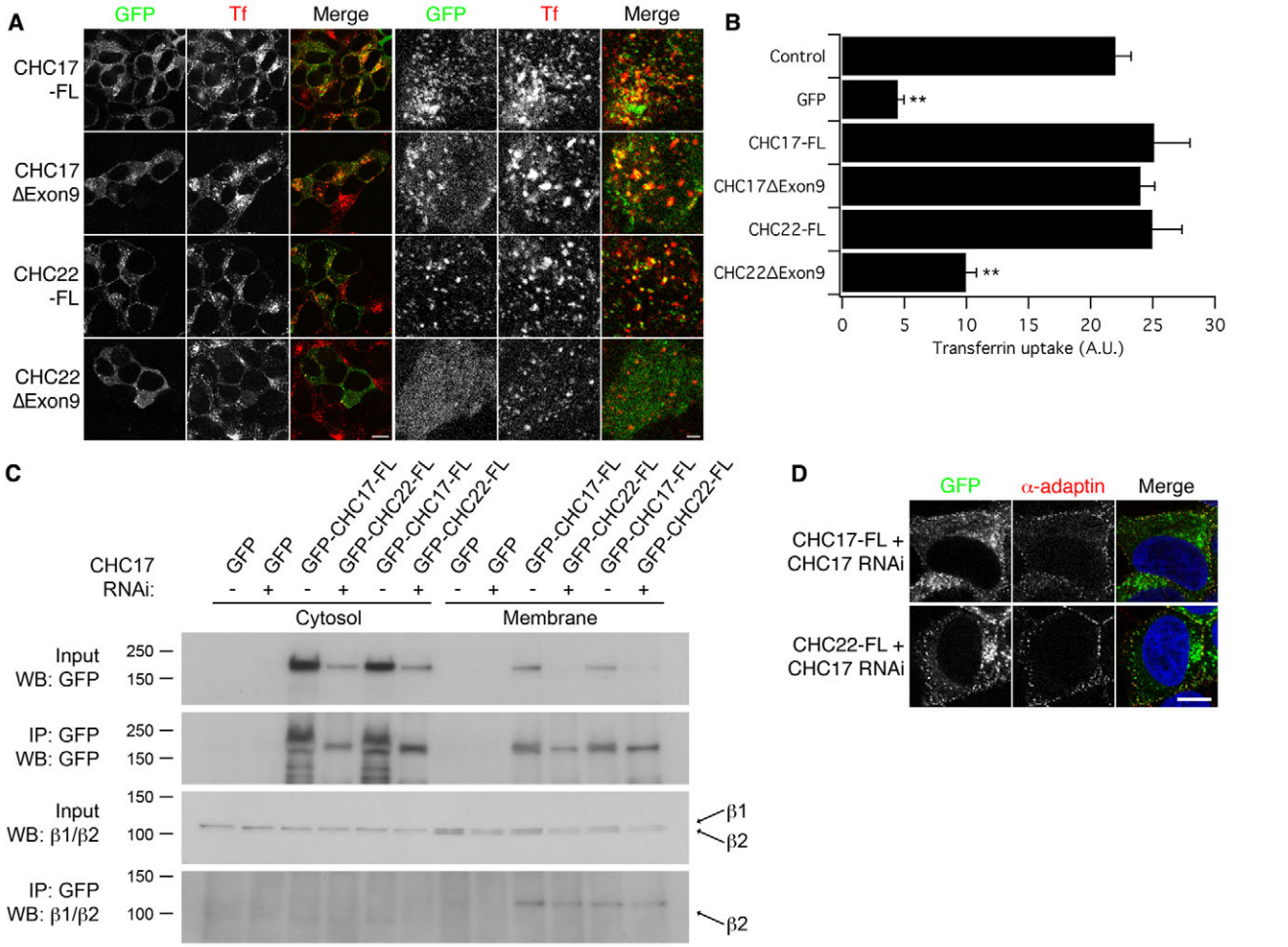

Fig. 3. Functional test for endocytosis in CHC17-depleted HEK293 cells expressing clathrin constructs. (A) Representative confocal micrographs to show relative distribution of GFP-tagged clathrin constructs (GFP, green in merge) and transferrin–Alexa-Fluor-546 (Tf, red in merge). Left panels give an indication of the rescue of clathrin-mediated endocytosis; right panels are confocal sections taken adjacent to the coverslip to visualise colocalisation of clathrin and transferrin spots. Scale bars: 10 µm (left); 2 µm (right). (B) Histogram to show mean ± s.e.m. transferrin uptake in CHC17-depleted HEK293 cells; n=3, $^{**}P$<0.01. (C) Co-immunoprecipitation of β2-adaptin with GFP–CHC17-FL and GFP–CHC22-FL. HEK293 cells transfected as described and immunoprecipitations of either the cytosolic or membrane-enriched fractions were done using anti-GFP. Samples of the inputs and IPs were analysed by western blotting for GFP or β1 and β2 adaptin. Under the conditions of our experiments, equivalent amounts of β1- and β2-adaptin are present in the membrane-enriched fraction, but only β2-adaptin co-immunoprecipitated with CHCs. Western blots (WBs) were typical of three experiments. Molecular masses (kDa) are as indicated to the left. (D) Representative confocal micrographs to show colocalisation of GFP–CHC22-FL or GFP–CHC17-FL (green) with α-adaptin detected with AP.6/A546 (red). Cells were depleted of endogenous CHC17 by RNAi. DAPI (DNA) is blue in the merged image. Scale bar: 10 µm.

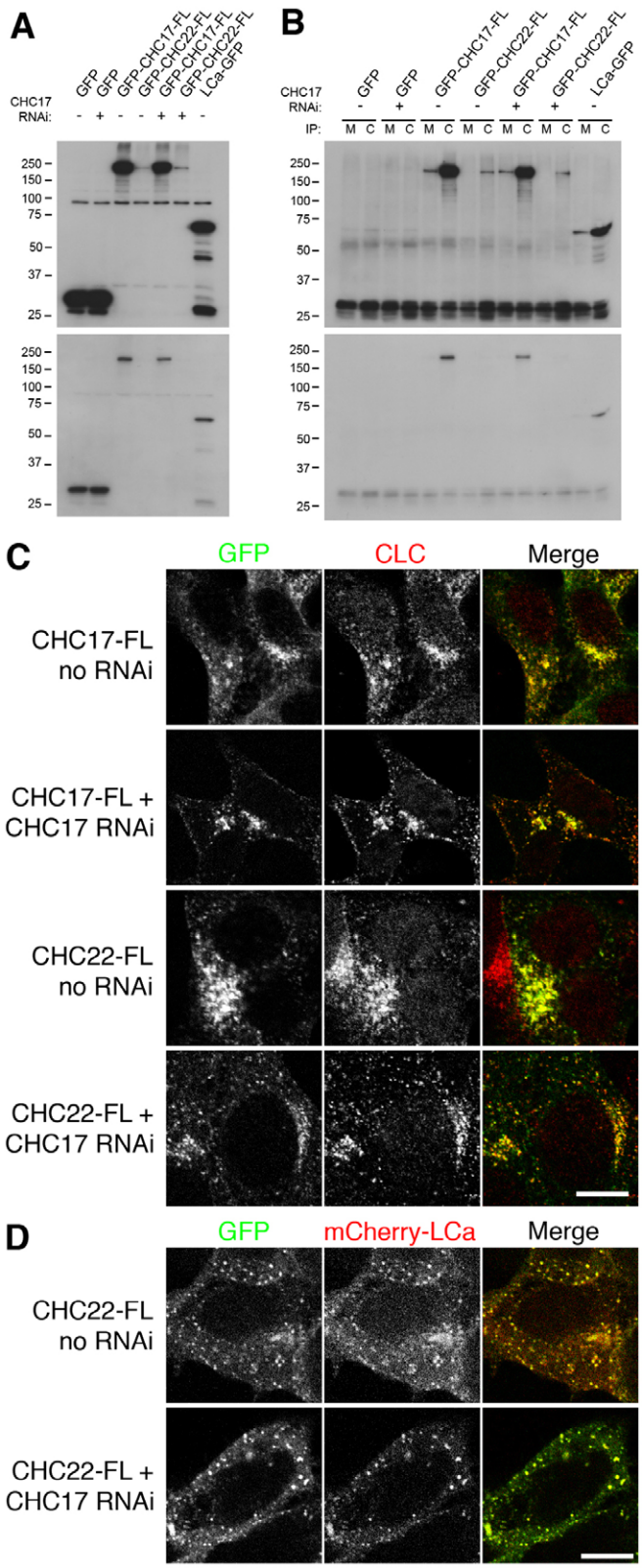

Fig. 4. Association between CHC22 and clathrin light chains. (A,B) IPs were performed using either anti-Myc (M) or anti-clathrin light chain (C) from lysates of HEK293 cells transfected as indicated. Samples of the lysates (A) or the IP (B) were analysed by blotting for GFP. Long (top) and short (bottom) exposures are shown to visualise the signal for GFP–CHC22-FL. These blots are typical of three experiments. (C) Representative confocal micrographs of cells expressing GFP–CHC17-FL or GFP–CHC22-FL (green) in the presence (no RNAi) or near absence (CHC17 RNAi) of endogenous CHC17. Cells were stained for endogenous clathrin light chains using CON.1/A546 (CLC, red). (D) Representative confocal micrographs of cells expressing GFP–CHC22-FL (left, green in merge) and mCherry-LCa (middle, red in merge) in the presence (no RNAi) or near absence (CHC17 RNAi) of endogenous CHC17. Scale bars: 10 μm.

in the interaction between CHC17 and proteins containing clathrin-box motifs are completely conserved in CHC22; therefore, we would predict that such interactions are equivalent. Our functional data provide strong evidence that CHC22 can interact with AP2, because transferrin-receptor endocytosis is AP2-dependent (Jing et al., 1990; Nesterov et al., 1999; Hinrichsen et al., 2003; Motley et al., 2003). To confirm that this was indeed the case, we tested for such an interaction biochemically by immunoprecipitation (IP) of GFP-tagged CHCs from membrane-enriched fractions and western blotting to detect β1- and β2-adaptin using a monoclonal antibody, 100/1 (Fig. 3C). Under the conditions of our experiments, we found that β2-adaptin was co-immunoprecipitated by GFP–CHC17-FL and by GFP–CHC22-FL. The interaction was evident irrespective of depletion of endogenous CHC17 (Fig. 3C). In support of these results, cells expressing GFP–CHC22-FL, but depleted of CHC17, that were co-stained for α-adaptin had a subset of GFP spots that colocalised with α-adaptin puncta. The colocalisation was similar to that seen for GFP–CHC17-FL under the same conditions (Fig. 3D). These observations indicate that CHC22-mediated endocytosis is similar to that mediated by CHC17, and that CHC22, similar to CHC17, can indeed interact with AP2. We interpret the earlier report of a lack of interaction between AP2 and CHC22 in HeLa cells as an out-competition of binding by the high levels of CHC17 relative to CHC22.

We finally set out to determine whether or not CHC22-FL can associate with clathrin light chains, as there have been conflicting reports on this issue (Liu et al., 2001; Towler et al., 2004b). To analyse binding between endogenous clathrin light chains and GFP-tagged CHCs, co-immunoprecipitation experiments were performed on HEK293 cells expressing GFP–CHC17-FL or GFP–CHC22-FL, using a monoclonal anti-clathrin-light-chain antibody, CON.1 (Fig. 4A-B). Analysis of the lysates used for IPs indicated that there was a large difference in expression between GFP–CHC17-FL and GFP–CHC22-FL (Fig. 4A), reflecting the lower transfection rate and expression of CHC22-FL compared with CHC17-FL. Nonetheless, we detected specific co-immunoprecipitation of GFP–CHC22-FL with clathrin light chains (Fig. 4B). This indicated a biochemical association between CHC22 and clathrin light chains. We next observed, by confocal microscopy, good colocalisation between GFP–CHC22-FL and endogenous clathrin light chains. The colocalisation was similar to that for GFP–CHC17-FL and also did not noticeably differ with or without CHC17 RNAi (Fig. 4C). We also observed virtually complete colocalisation of GFP–CHC22-FL coexpressed with mCherry-tagged clathrin light chain a (LCa). The colocalisation of puncta was again independent of CHC17 levels (Fig. 4D). These results suggest that CHC22, similar to CHC17, can indeed associate with clathrin light chains in cells.

The observation of functional equivalence between CHC17-FL and CHC22-FL reported here is only of significance if CHC22-FL is actually expressed endogenously. To investigate which form of CHC22 is expressed, we cloned DNA encoding CHC22 from human skeletal-muscle cDNA and from HeLa cDNA (supplementary

Journal of Cell Science

Journal of Cell Science

material Fig. S2). We found expression of full-length CHC22 only, i.e. the exon-9-containing form. A transcript encoding CHC22 that lacked exon 9 is expressed, but only in a truncated form that terminates downstream of exon 10 and upstream of exon 27. This means that, if translation does occur, this variant would not form triskelia and would be unlikely to function as anything other than a dominant-negative. We also found no evidence for the alternative splicing of exon 9 in CHC17 (supplementary material Fig. S2). The implication is that the CHC22 form that has previously been studied (Liu et al., 2001; Towler et al., 2004b) is a variant that is not normally found in skeletal muscle or HeLa cells. This is further compounded by the observation that CHC22ΔExon9 is non-functional in the assays used here.

One potential concern with our experimental strategy is that the functional rescue that we observed might be due to the association of non-functional CHCs with the trace amounts of endogenous CHC17 left in cells following RNAi. We believe that this is unlikely because CHC22 does not appear to co-trimerise with CHC17 (Liu et al., 2001) and even transfected CHC17 does not co-trimerise with endogenous CHC17 (Liu et al., 1998; Wilde et al., 1999). In addition, we have expressed, under the same RNAi conditions, a CHC17 lacking the N-terminal domain necessary for binding to AP2 and found no functional rescue of endocytosis (Royle and Lagnado, 2006). This indicates that, in our experimental system, the CHCs that are transfected can form triskelia that operate independently of trace amounts of CHC17.

In summary, when expressed under similar conditions, CHC17 and CHC22 are equally functional in endocytosis and mitosis. In most cells in the body, the level of CHC22 expression is apparently too low for a significant contribution to endocytosis or mitosis, and this explains why endocytic and mitotic defects are actually observed upon CHC17 depletion (Hinrichsen et al., 2003; Motley et al., 2003; Royle et al., 2005). The ability of CHC22 to functionally substitute for CHC17 is likely to be relevant in cells expressing higher levels of CHC22, such as in skeletal muscle, especially during myogenesis when CHC22 expression is further enhanced (Liu et al., 2001; Towler et al., 2004b). We also do not rule out the possibility that CHC22 has unique functions. For example, CHC22, unlike CHC17, can bind to sorting nexin 5 (SNX5), a membrane-trafficking protein that is enriched in skeletal muscle (Towler et al., 2004b).

The present work provides further support to the idea that the mitotic function of clathrin is separate from the function of clathrin in endocytosis. We have previously showed that: (1) a dominant-negative construct that interferes with endocytosis does not cause mitotic defects as a secondary effect (Royle et al., 2005), (2) mitosis can be rescued partially in CHC17-depleted cells by a construct that is not competent for endocytosis [stunted construct (Royle and Lagnado, 2006)]. Here, we found that CHC17ΔExon9 is a construct that can rescue endocytosis but not mitosis in CHC17-depleted cells. This further suggests that these two functions for clathrin are separable. Another interesting observation from this work is that removal of exon 9 from either CHC17 or CHC22 resulted in a reduction of spindle-binding. This raises the possibility that the residues encoded by exon 9, in addition to the N-terminal domain, constitute a binding site for microtubules or microtubule-associated proteins of spindle fibres. Alternatively, the removal of CHCR0 helices e-h might result in a conformational change that results in the N-terminal domains no longer being available for spindle-binding (supplementary material Fig. S1). These two models are currently being tested in our laboratory.

Materials and Methods

Molecular biology

DNA constructs

A plasmid containing human CHC22ΔExon9 (in pEGFP-N3) was a gift from Frances Brodsky (UCSF) (Towler et al., 2004b). In order to make GFP-CHC22ΔExon9, a *Hin*dIII-*Xma*I fragment from the pEGFP-N3 plasmid was subcloned into pEGFP-C1. This gave GFP-CHC22ΔExon9 with an extra 7 amino acids (GPSTGSR) before the stop codon. Chimeric clathrin constructs were made by first inserting restriction sites that are present in CHC17 into GFP-CHC22ΔExon9 by site-directed mutagenesis and then swapping fragments between these plasmids and human GFP–CHC17-FL (Royle and Lagnado, 2006).

GFP–CHC22-FL was made by 'repairing' GFP-CHC22ΔExon9 by inserting a *Sca*I-*Bsp*EI fragment digested from an internal PCR from human testis cDNA library (Clontech). GFP-CHC17ΔExon9 was made by overlap extension PCR using GFP-CHC17(1-1675)KDP as template and *Acc*65I-*Sal*I sites.

pBrain-GFP-CHC(1-1675)KDP-CHC4 was available from previous work (Royle and Lagnado, 2006). We made pBrain-GFP-CHC17ΔExon9-CHC4 by inserting a *Bgl*II-*Eco*RV fragment from GFP-CHC17ΔExon9 into pBrain-GFP-CHC(1-1675)KDP-CHC4. The pBrain-GFP-CHC22FL-CHC4 and pBrain-GFP-CHC22ΔExon9-CHC4 were made by inserting an *Apa*LI-*Age*I fragment from pBrain-GFP-CHC4 into GFP-CHC22FL and GFP-CHC22ΔExon9. Any constructs that contained the sequence coding for CHC17 residues 60-66 were knockdown-proof (Royle et al., 2005). CHC22 has four changes from the CHC17 shRNA target sequence and was therefore not targeted by RNAi. All constructs were verified by restriction digest and any that involved PCR were further verified by automated DNA sequencing (Geneservice, UK).

Amplification and analysis of CHC22 and CHC17 transcripts

Total RNA from HeLa and HEK293 cells was extracted using Trizol (Invitrogen), human skeletal-muscle total RNA (No. 540029) was from Stratagene. In each case, cDNA was obtained from 5 μg total RNA using an oligo dT_{15} primer and amplified with Superscript II reverse transcriptase (Invitrogen). Following first-strand cDNA synthesis, the hybridised mRNA was degraded using RNAse H. Amplification from these cDNA templates was by PCR using PfuTurbo (Stratagene). Details of primers used are given in supplementary material Table S1.

Cell biology

HEK293 cell culture, transfection, transferrin uptake and immunocytochemistry were carried out as described previously (Royle and Lagnado, 2006). The RNAi conditions for rescue experiments have been described elsewhere (Royle and Lagnado, 2006). In summary, we typically get >90% reduction of CHC17 compared with controls at 72 hours and re-expression levels of GFP-CHC17 are approximately two-thirds of endogenous CHC17 levels. Here, the fluorescence intensity of GFP–CHC22-FL was less than that of GFP–CHC17-FL and the transfection rate of GFP–CHC22-FL was also consistently lower than GFP–CHC17-FL. Monoclonal antibodies used were: anti-Myc (9E10, Zymed laboratories, 13-2500), anti-CHC17 (TD.1, Covance, MMS-427P), anti-clathrin-light-chain (CON.1, Sigma Aldrich, C1985), anti-β1/β2-adaptin (100/1, AbCam, ab11327) and anti-α-adaptin (AP.6, Cambridge Bioscience, MA1-064). Polyclonal sheep anti-GFP was a generous gift of Francis Barr (University of Liverpool, UK). For immunoblotting, antibody concentrations were as follows: 49.5 μg/ml 100/1, 1 μg/ml TD.1, 1:1000 anti-GFP. Anti-mouse HRP-conjugated IgG (GE Healthcare, 1:10,000) and anti-sheep HRP-conjugated IgG (Cambridge Bioscience, 1:10,000) were use for detection. For immunocytochemistry, 5 μg/ml CON.1 and 25 μg/ml AP6 was used. Anti-mouse Alexa-Fluor-546-conjugated IgG (Invitrogen, 1:500) was used for detection.

Biochemistry

HEK293 cells transfected with GFP-clathrin constructs or control plasmids were harvested 72 hours post-transfection. The fractionation protocol was as described elsewhere (McCullough et al., 2006). Briefly, cells were homogenised in homogenisation buffer (10 mM HEPES, pH 7.2, 3 mM imidazole, 250 mM sucrose, protease inhibitor cocktail) by passing through a 23G needle six to eight times. Nuclei were spun out of the homogenate at 1900 ***g***, and the post-nuclear supernatant spun at 100,000 ***g*** in a Beckman TLA120.2 rotor to separate the cytosolic supernatant from the membrane-enriched pellet.

For whole-cell lysates, transfected HEK293 cells were trypsinised and resuspended in lysis buffer A (20 mM Tris, pH 7.5, 150 mM NaCl, 1% IGEPAL, 30 mM NaF, 5 mM Na_3VO_4, 15 μg/ml DNase I, 100 nM okadaic acid, protease inhibitor cocktail), incubated on ice for 30 minutes, then spun at 20,000 ***g*** at 4°C for 15 minutes. The supernatant was retained as cell lysate. For IPs, 1 mg lysate per IP was pre-cleared with 10 μl protein G beads for 1 hour at 4°C, rotating, then incubated with either 3 μl GFP antibody or 2 μg CON.1 or 9E10 antibody for 1 hour at 4°C, rotating. Then, 15 μl protein G beads were added and incubated for a further 1.5 hours at 4°C, rotating, in the case of CON.1 IPs, or overnight at 4°C, rotating, for GFP IPs. Beads were washed once with 1 ml lysis buffer B (20 mM Tris, pH 7.5, 150 mM NaCl, 1% IGEPAL, protease inhibitor cocktail), and four times with 1 ml wash buffer (20 mM Tris, pH 7.5, 150 mM NaCl, 0.1% IGEPAL, protease inhibitor cocktail). Beads were resuspended in Laemmli buffer.

Imaging and data analysis

Confocal imaging was done using a Leica confocal microscope SP2 with a 63× (1.4 NA) oil-immersion objective. GFP, Alexa Fluor 546 and mCherry were excited using an Ar/Kr 488 nm laser, a He/Ne 543 nm laser or He/Ne 543/594 nm laser lines, respectively. H33342 or DAPI were excited using a multiphoton laser. Excitation and collection of emission were performed separately and sequentially. For quantitative experiments, identical laser power and acquisition settings were used. For analysis of transferrin uptake, images were imported into ImageJ (NIH), the outline of the cell was manually drawn using the GFP channel as a guide and this ROI was transferred to the red channel. The image was thresholded and the transferrin–Alexa-Fluor-546 puncta quantified. Experiments to determine the mitotic index were quantified by counting the number of GFP-positive cells with mitotic figures as a proportion of the total number of GFP-positive cells within an area of 1.215 mm^2. The number of GFP-positive metaphase-like cells that contained misaligned chromosomes was counted. For mitotic-index measurements between 1026 and 2113 cells per condition were counted. For transferrin uptake measurements, between 78 and 99 cells were analysed for each condition. All experiments were preformed three or more times. Normally distributed data were analysed by ANOVA with Dunnet's post-hoc test and binomial data were analysed by Chi-squared approximation using Instat (Graphpad). Figures were assembled using Igor Pro (Wavemetrics), PyMOL (DeLano Scientific) and Adobe Photoshop.

We thank Hannah Dunford for technical assistance during the early stages of this study; Frances Brodsky for the gift of CHC22ΔExon9-GFP; and Francis Barr and Ulrike Gruneberg for helpful suggestions and useful reagents. We thank Sylvie Urbé for help with preparing membrane-enriched fractions. This work was supported by a Career Establishment Award from Cancer Research UK.

References

Borner, G. H., Harbour, M., Hester, S., Lilley, K. S. and Robinson, M. S. (2006). Comparative proteomics of clathrin-coated vesicles. *J. Cell Biol.* **175**, 571-578.

Dell'Angelica, E. C., Klumperman, J., Stoorvogel, W. and Bonifacino, J. S. (1998). Association of the AP-3 adaptor complex with clathrin. *Science* **280**, 431-434.

Drake, M. T. and Traub, L. M. (2001). Interaction of two structurally distinct sequence types with the clathrin terminal domain beta-propeller. *J. Biol. Chem.* **276**, 28700-28709.

Fotin, A., Cheng, Y., Sliz, P., Grigorieff, N., Harrison, S. C., Kirchhausen, T. and Walz, T. (2004). Molecular model for a complete clathrin lattice from electron cryomicroscopy. *Nature* **432**, 573-579.

Gong, W., Emanuel, B. S., Collins, J., Kim, D. H., Wang, Z., Chen, F., Zhang, G., Roe, B. and Budarf, M. L. (1996). A transcription map of the DiGeorge and velo-cardio-facial syndrome minimal critical region on 22q11. *Hum. Mol. Genet.* **5**, 789-800.

Hinrichsen, L., Harborth, J., Andrees, L., Weber, K. and Ungewickell, E. J. (2003). Effect of clathrin heavy chain- and alpha-adaptin-specific small inhibitory RNAs on endocytic accessory proteins and receptor trafficking in HeLa cells. *J. Biol. Chem.* **278**, 45160-45170.

Jing, S. Q., Spencer, T., Miller, K., Hopkins, C. and Trowbridge, I. S. (1990). Role of the human transferrin receptor cytoplasmic domain in endocytosis: localization of a specific signal sequence for internalization. *J. Cell Biol.* **110**, 283-294.

Kedra, D., Peyrard, M., Fransson, I., Collins, J. E., Dunham, I., Roe, B. A. and Dumanski, J. P. (1996). Characterization of a second human clathrin heavy chain polypeptide gene (CLH-22) from chromosome 22q11. *Hum. Mol. Genet.* **5**, 625-631.

Kirchhausen, T. (2000). Clathrin. *Annu. Rev. Biochem.* **69**, 699-727.

Lindsay, E. A., Rizzu, P., Antonacci, R., Jurecic, V., Delmas-Mata, J., Lee, C. C., Kim, U. J., Scambler, P. J. and Baldini, A. (1996). A transcription map in the CATCH22 critical region: identification, mapping, and ordering of four novel transcripts expressed in heart. *Genomics* **32**, 104-112.

Liu, S. H., Marks, M. S. and Brodsky, F. M. (1998). A dominant-negative clathrin mutant differentially affects trafficking of molecules with distinct sorting motifs in the class II major histocompatibility complex (MHC) pathway. *J. Cell Biol.* **140**, 1023-1037.

Liu, S. H., Towler, M. C., Chen, E., Chen, C. Y., Song, W., Apodaca, G. and Brodsky, F. M. (2001). A novel clathrin homolog that co-distributes with cytoskeletal components functions in the trans-Golgi network. *EMBO J.* **20**, 272-284.

Long, K. R., Trofatter, J. A., Ramesh, V., McCormick, M. K. and Buckler, A. J. (1996). Cloning and characterization of a novel human clathrin heavy chain gene (CLTCL). *Genomics* **35**, 466-472.

Maro, B., Johnson, M. H., Pickering, S. J. and Louvard, D. (1985). Changes in the distribution of membranous organelles during mouse early development. *J. Embryol. Exp. Morphol.* **90**, 287-309.

McCullough, J., Row, P. E., Lorenzo, O., Doherty, M., Beynon, R., Clague, M. J. and Urbe, S. (2006). Activation of the endosome-associated ubiquitin isopeptidase AMSH by STAM, a component of the multivesicular body-sorting machinery. *Curr. Biol.* **16**, 160-165.

Miele, A. E., Watson, P. J., Evans, P. R., Traub, L. M. and Owen, D. J. (2004). Two distinct interaction motifs in amphiphysin bind two independent sites on the clathrin terminal domain beta-propeller. *Nat. Struct. Mol. Biol.* **11**, 242-248.

Motley, A., Bright, N. A., Seaman, M. N. and Robinson, M. S. (2003). Clathrin-mediated endocytosis in AP-2-depleted cells. *J. Cell Biol.* **162**, 909-918.

Nesterov, A., Carter, R. E., Sorkina, T., Gill, G. N. and Sorkin, A. (1999). Inhibition of the receptor-binding function of clathrin adaptor protein AP-2 by dominant-negative mutant mu2 subunit and its effects on endocytosis. *EMBO J.* **18**, 2489-2499.

Okamoto, C. T., McKinney, J. and Jeng, Y. Y. (2000). Clathrin in mitotic spindles. *Am. J. Physiol. Cell Physiol.* **279**, C369-C374.

Royle, S. J. (2006). The cellular functions of clathrin. *Cell Mol. Life Sci.* **63**, 1823-1832.

Royle, S. J. and Lagnado, L. (2006). Trimerisation is important for the function of clathrin at the mitotic spindle. *J. Cell Sci.* **119**, 4071-4078.

Royle, S. J., Bright, N. A. and Lagnado, L. (2005). Clathrin is required for the function of the mitotic spindle. *Nature* **434**, 1152-1157.

Sirotkin, H., Morrow, B., DasGupta, R., Goldberg, R., Patanjali, S. R., Shi, G., Cannizzaro, L., Shprintzen, R., Weissman, S. M. and Kucherlapati, R. (1996). Isolation of a new clathrin heavy chain gene with muscle-specific expression from the region commonly deleted in velo-cardio-facial syndrome. *Hum. Mol. Genet.* **5**, 617-624.

ter Haar, E., Harrison, S. C. and Kirchhausen, T. (2000). Peptide-in-groove interactions link target proteins to the beta-propeller of clathrin. *Proc. Natl. Acad. Sci. USA* **97**, 1096-1100.

Towler, M. C., Kaufman, S. J. and Brodsky, F. M. (2004a). Membrane traffic in skeletal muscle. *Traffic* **5**, 129-139.

Towler, M. C., Gleeson, P. A., Hoshino, S., Rahkila, P., Manalo, V., Ohkoshi, N., Ordahl, C., Parton, R. G. and Brodsky, F. M. (2004b). Clathrin isoform CHC22, a component of neuromuscular and myotendinous junctions, binds sorting nexin 5 and has increased expression during myogenesis and muscle regeneration. *Mol. Biol. Cell* **15**, 3181-3195.

Wakeham, D. E., Abi-Rached, L., Towler, M. C., Wilbur, J. D., Parham, P. and Brodsky, F. M. (2005). Clathrin heavy and light chain isoforms originated by independent mechanisms of gene duplication during chordate evolution. *Proc. Natl. Acad. Sci. USA* **102**, 7209-7214.

Wilde, A., Beattie, E. C., Lem, L., Riethof, D. A., Liu, S. H., Mobley, W. C., Soriano, P. and Brodsky, F. M. (1999). EGF receptor signaling stimulates SRC kinase phosphorylation of clathrin, influencing clathrin redistribution and EGF uptake. *Cell* **96**, 677-687.

Journal of Cell Science